

THE INTERIOR ACOUSTIC-STRUCTURE COUPLED PROBLEM

Leonardo Molisani^a

^a*Grupo de Acústica y Vibraciones, Facultad de Ingeniería, Universidad Nacional de Río Cuarto, Ruta 36 Km 601, 5800 Río Cuarto, Argentina, lmolisani@ing.unrc.edu.ar*

Keywords: Interior Acoustics, Acoustic-Structure Coupling, Adjoint Problem.

Abstract. The goal of this effort is to solve the acoustic-structural coupling problem. To account for the inner acoustic cavity in the structural response, an expression for the acoustic pressure produced by the motion of the external structure is derived in this effort. To this end, the acoustic mode shapes and natural frequencies of the inner cavity are computed. The eigenproperties are then used to solve for the Green's functions, which allows to compute the acoustic pressure due to the structural motion. The modeling of the acoustic cavity is included in the structural. The structural model is evaluated numerically and validated by comparison to experimental results from the open literature. It is shown in this work that the acoustic cavity dynamics effect results in a sharp increase of the response around the shell cavity resonance.

INTRODUCTION

The problem here is to obtain an expression for the acoustic pressure induced by the structure motion. The acoustic cavity pressure in turn affects the structure response. In Figure 1, the general problem of finding the acoustic pressure in an structural enclosure is presented.

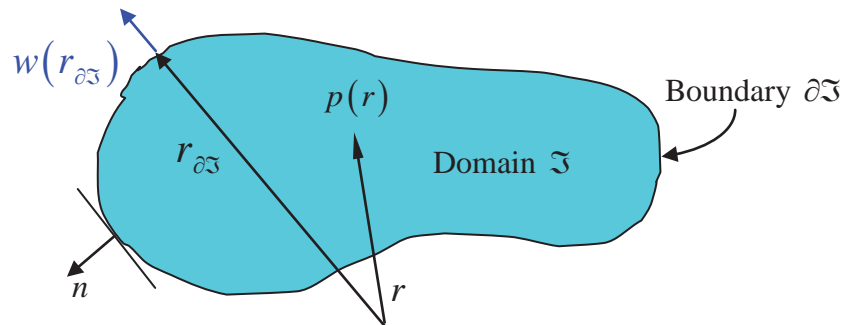


Figure 1: Interior acoustic problem.

The acoustic cavity is the volume \mathfrak{V} defined by the elastic boundary $\partial\mathfrak{V}$. The motion of the boundary is given by the velocity $w(r_{\partial\mathfrak{V}})$ in the normal direction n to the surface creates the acoustic pressure $p(r)$. Before addressing the general problem of finding $p(r)$, a discussion on the general boundary conditions for this type of problem is presented. The boundary conditions on the domain surface $\partial\mathfrak{V}$, i.e. inside cavity surface, can be expressed as

$$\alpha p(r) + \beta \frac{\partial p(r)}{\partial n} \Big|_{\partial\mathfrak{V}} = B(r), \quad \text{on } \partial\mathfrak{V} \quad (1)$$

Where n is the normal to the boundary $\partial\mathfrak{V}$, $p(r)$ the acoustic pressure and α, β , and B are given functions evaluated on the region $\partial\mathfrak{V}$. The boundary condition relates the values of $p(r)$ on $\partial\mathfrak{V}$ and the flux of $p(r)$ through $\partial\mathfrak{V}$. The condition of $\alpha \geq 0, \beta \geq 0$ and $\alpha + \beta > 0$ on $\partial\mathfrak{V}$ are required (Zauderer, 1989). If $\alpha \neq 0$ and $\beta = 0$, the boundary condition is called of the *first kind* or *Dirichlet condition*. If $\alpha = 0$ and $\beta \neq 0$, the boundary condition is called of the *second kind* or *Neumann condition*. If $\alpha \neq 0$ and $\beta \neq 0$, the boundary condition is called of the *third kind* or *mixed kind*. When B does not vanish, the boundary conditions are of inhomogeneous type. If B and α vanish at the boundary the condition is “hard wall”.

Consider now a general differential operator L and

$$Lp(r) = F(r) \quad \text{in } \mathfrak{V} \quad (2)$$

Where $F(r)$ represent the external influences on the system. The operator L is not assumed to be formally self-adjoint, $L \neq L^*$ in order to keep the richness in the development. Therefore, the adjoint operator L^* of L satisfies the equation (Roach, 1970)

$$LG(r|r_o) = \delta(r-r_o) \quad (3)$$

Where $G(r|r_o)$ is the Green's function. The boundary condition are given by the adjoint of the operator $B(r)$. The inner product upon the domain \mathfrak{V} is defined as

$$\langle x, y \rangle = \int_{\mathfrak{V}} x \bar{y} d\mathfrak{V} \quad (4)$$

Where the over-bar in equation (4) denotes complex conjugates (Naylor and Sell, 2000). Taking the inner product on equation (2) with the Green's function $G(r|r_o)$, it gives

$$\langle G(r|r_o), Lp(r) \rangle = \langle G(r|r_o), F(r) \rangle \quad (5)$$

and again the inner product on equation (3) by $p(r)$, it yields

$$\langle p(r), LG(r|r_o) \rangle = \langle p(r), \delta(r-r_o) \rangle \quad (6)$$

Subtracting equation (6) from(5), the following relation holds

$$\langle G(r|r_o), Lp(r) \rangle - \langle p(r), LG(r|r_o) \rangle = \langle G(r|r_o), F(r) \rangle - \langle p(r), \delta(r-r_o) \rangle \quad (7)$$

or

$$\int_{\mathfrak{V}} [G(r|r_o) \overline{Lp(r)} - p(r) \overline{LG(r|r_o)}] d\mathfrak{V} = \int_{\mathfrak{V}} [G(r|r_o) \overline{F(r)} - p(r) \overline{\delta(r-r_o)}] d\mathfrak{V} \quad (8)$$

Using the following properties of the three-dimensional Dirac delta

$$\int_{\mathfrak{V}} p(r) \overline{\delta(r-r_o)} d\mathfrak{V} = \begin{cases} p(r_o), & r_o \text{ within } \mathfrak{V} \\ \frac{1}{2} p(r_o), & r_o \text{ on } \partial\mathfrak{V} \\ 0, & r_o \text{ outside of } \mathfrak{V} \end{cases} \quad (9)$$

the expression for the acoustic pressure is given by

$$p(r_o) = \varepsilon_{\mathfrak{V}} \int_{\mathfrak{V}} [G(r|r_o) \overline{F(r)} + p(r) \overline{LG(r|r_o)} - G(r|r_o) \overline{Lp(r)}] d\mathfrak{V} \quad (10)$$

where

$$\varepsilon_{\mathfrak{V}} = \begin{cases} 1, & r_o \text{ within } \mathfrak{V} \\ 2, & r_o \text{ on } \partial\mathfrak{V} \end{cases} \quad (11)$$

Equation (10) becomes

$$p(r_o) = \varepsilon_{\mathfrak{V}} \int_{\mathfrak{V}} [p(r) \overline{LG(r|r_o)} - G(r|r_o) \overline{Lp(r)}] d\mathfrak{V} \quad (12)$$

The integrand of equation (12) is a divergence expression where L is the *formally adjoint operator* of L . Moreover if $L=L$, the operator L is *formally self-adjoint*. The boundary condition associated to the given equation and its formal adjoint boundary condition play an

important role to determine whether or not the problem is self-adjoint. Therefore, it is possible for an operator to be formally self adjoint but for the problem associated with this operator and its adjoint to be nonself-adjoint. But if the operator is not self-adjoint the problem cannot be self adjoint. Equation (12) is a general expression for the acoustic pressure. Further development requires specifying the character of the operator L used to model the acoustic problem.

1 APPLICATION: THE CILINDRICAL ACOUSTIC CAVITY

The operator for this particular application is given by the linear wave equation, which is self-adjoint ($L = L$). That is

$$\nabla^2 p - \frac{1}{c^2} \frac{d^2 p}{dt^2} = 0 \quad (13)$$

with boundary condition

$$\left. \frac{\partial p(r)}{\partial n} \right|_{\partial \mathfrak{V}} = -\rho \frac{\partial w(r)}{\partial t} \quad \text{with } r \in \partial \mathfrak{V} \quad (14)$$

where $w(r)$ is the velocity at the boundary and p is assumed to have the form

$$p(r, \theta, x, t) = p(r, \theta, x) e^{i\omega t} \quad (15)$$

Since the boundary conditions is harmonic, replacing equation (15) into (13) and (14), the resultant equations is given by

$$\nabla^2 p + k^2 p = 0 \quad \text{and} \quad \left. \frac{\partial p(r)}{\partial n} \right|_{\partial \mathfrak{V}} = -i\omega\rho w(r) \quad \text{with } r \in \partial \mathfrak{V} \quad (16)$$

this equation is the so called Helmholtz equation, in where k is the free field acoustic wavenumber. Then, using equation (12) the acoustic pressure becomes

$$p(r_o) = \varepsilon_{\mathfrak{V}} \int_{\mathfrak{V}} \left\{ p(r) [\nabla^2 G(r|r_o) + k^2 G(r|r_o)] - G(r|r_o) [\nabla^2 p(r) + k^2 p(r)] \right\} d\mathfrak{V} \quad (17)$$

with $r \in \partial \mathfrak{V}$

or

$$p(r_o) = \varepsilon_{\mathfrak{V}} \int_{\mathfrak{V}} \left\{ [p(r) \nabla^2 G(r|r_o) - G(r|r_o) \nabla^2 p(r)] + [p(r) k^2 G(r|r_o) - G(r|r_o) k^2 p(r)] \right\} d\mathfrak{V} \quad (18)$$

with $r \in \partial \mathfrak{V}$

The second term in the integral of equation (18) vanishes. The simplification in the inner product given in the integration is due to the self-adjoint property of the Helmholtz operator. Therefore, the operator left in equation (18) is the Laplace's operator, which also is self adjoint (Kreyszig, 1978). Then, it is possible to write

$$\begin{aligned}
 p(r_o) &= \varepsilon_{\mathfrak{V}} \int_{\mathfrak{V}} [p(r) \nabla^2 G(r|r_o) - G(r|r_o) \nabla^2 p(r)] d\mathfrak{V} \\
 &= \varepsilon_{\mathfrak{V}} \int_{\mathfrak{V}} \nabla \bullet [p(r) \nabla G(r|r_o) - G(r|r_o) \nabla p(r)] d\mathfrak{V} \\
 &\text{with } r \in \partial\mathfrak{V}
 \end{aligned}
 \tag{19}$$

Applying Gauss’s second identity on (19) (Griffel, 1985), it gives

$$\begin{aligned}
 p(r_o) &= \varepsilon_{\mathfrak{V}} \int_{\mathfrak{V}} \nabla \bullet [p(r) \nabla G(r|r_o) - G(r|r_o) \nabla p(r)] d\mathfrak{V} \\
 &= \varepsilon_{\mathfrak{V}} \int_{\partial\mathfrak{V}} n \bullet [p(r) \nabla G(r|r_o) - G(r|r_o) \nabla p(r)] d(\partial\mathfrak{V}) \\
 &= \varepsilon_{\mathfrak{V}} \int_{\partial\mathfrak{V}} \left[p(r) \frac{\partial G(r|r_o)}{\partial n} - G(r|r_o) \frac{\partial p(r)}{\partial n} \right] d(\partial\mathfrak{V}) \\
 &\text{with } r \in \partial\mathfrak{V}
 \end{aligned}
 \tag{20}$$

A Green’s function satisfying the “rigid wall” (Wu, 2000) condition implies that

$$\frac{\partial G(r|r_o)}{\partial n} = 0 \quad \text{on } r \in \partial\mathfrak{V}
 \tag{21}$$

Replacing the boundary condition given by equation (14) and the condition (21), the acoustic pressure produced by the motion of the boundary is given by

$$\begin{aligned}
 p(r_o) &= \varepsilon_{\mathfrak{V}} \int_{\partial\mathfrak{V}} i\omega\rho w(r) G(r|r_o) d(\partial\mathfrak{V}) \\
 &\text{with } r \in \partial\mathfrak{V}
 \end{aligned}
 \tag{22}$$

To find the acoustic pressure and thus the dynamics of the acoustic the hard wall Green’s function are needed. To this end, the eigenvalue problem associated to the operator for the hard wall boundary condition need to be solved. The eigenproperties are then used to construct the Green’s functions. Then, the Green’s function is used to compute the pressure inside the acoustic cavity due to the motion of the flexible shell using (22). The acoustic cavity is modeled as a cylindrical cavity with annular section as shown in Figure 2.

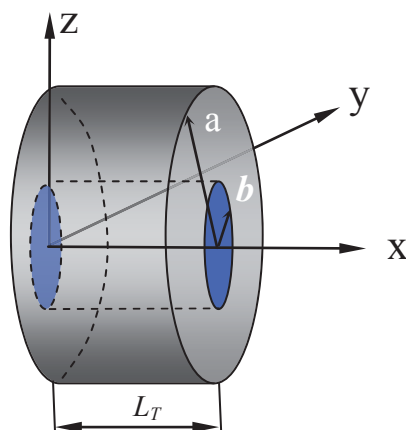


Figure 2: Finite annular cylindrical cavity.

Due to the geometry of the acoustic cavity, the Helmholtz equation is expressed in cylindrical coordinates as follow

$$\frac{\partial^2 p}{\partial r^2} + \frac{1}{r} \frac{\partial p}{\partial r} + \frac{1}{r^2} \frac{\partial^2 p}{\partial \theta^2} + \frac{\partial^2 p}{\partial x^2} + k^2 p = 0 \quad (23)$$

the rigid wall boundary conditions are of the *first kind* or *Dirichlet* conditions defined as

$$\left(\frac{\partial p}{\partial x} \right)_{x=0} = \left(\frac{\partial p}{\partial x} \right)_{x=L_T} = \left(\frac{\partial p}{\partial r} \right)_{r=a} = \left(\frac{\partial p}{\partial r} \right)_{r=b} = 0 \quad (24)$$

the acoustic pressure p is assumed to be the solution of equation (23) in the form

$$p(r, \theta, x, t) = p(r, \theta, x) e^{i\omega_{qpl} t} = \hat{A}_{qpl} \Psi_{qpl}(r, \theta, x) e^{i\omega_{qpl} t} \quad (25)$$

where $\Psi_{qpl}(r, \theta, x)$ is the acoustic pressure mode shape corresponding to the natural angular frequency ω_{qpl} and \hat{A}_{qpl} is the acoustic modal amplitude. The three indexes used in the acoustic pressure mode shapes have the following meaning:

- q is the mode index on the axial direction.
- p index is the acoustic mode order on the azimuth direction, which also couples with the radial direction for the cylindrical cavity.
- l index represents the mode order in the radial direction.

Replacing equation (25) into (23), the solution of equation (23) under the boundary conditions (24) is

$$\Psi_{qpl}(r, \theta, x) = \left[Y'_p(k_{pl}a) J_p(k_{pl}r) - J'_p(k_{pl}a) Y_p(k_{pl}r) \right] \cos(p\theta) \cos(k_{xq}x) \quad (26)$$

with $q, p, l = 0, 1, 2, \dots$

where J_p and Y_p are the Bessel's functions of First and Second Kind, respectively (Watson, G., 1958); k_{pl} is the radial wavenumber which couples with the azimuth direction, and k_{xq} is the wavenumber associated to the axial direction. The eigen-wavenumber of the Helmholtz operator is given by

$$k_{qpl} = \frac{\omega_{qpl}}{c} = \frac{2\pi f_{qpl}}{c} \cong \sqrt{k_{xq}^2 + k_{pl}^2} = \sqrt{\left(\frac{l\pi}{a-b} \right)^2 + \left(\frac{2p}{a+b} \right)^2 + \left(\frac{q\pi}{L_T} \right)^2} \quad (27)$$

The eigenfunction $\Psi_{qpl}(r, \theta, x)$ satisfies the following orthogonality property

$$\int_0^{2\pi} \int_0^{L_T} \int_b^a \Psi_{qpl}(x, \theta, r) \Psi_{rso}(x, \theta, r) r dr dx d\theta = \Lambda_{qpl} \delta_{qr} \delta_{ps} \delta_{lo} \quad (28)$$

Where Λ_{qpl} is the mode normalization factor. For example, the Figure 3 shows the Ψ_{010}

acoustic mode shape. This acoustic mode shape is highlighted because it is the one that couples with the structure in the low frequency range. Only this acoustic mode is analyzed in this effort because it is the culprit of the vertical excitation of the shell structure. Moreover, a harmonic point force acting in the shell structure is capable only to excite this acoustic mode due to the symmetry of the problem. The mode shape Ψ_{010} has variation along the azimuth direction θ ($\cos(p\theta)$), while the values in the radial direction are “almost constant”, i.e. only a 2.5% of variation in the acoustic pressure from $r = a$ to $r = b$. Therefore, the radial sections can be assumed constant without much loss of generality.

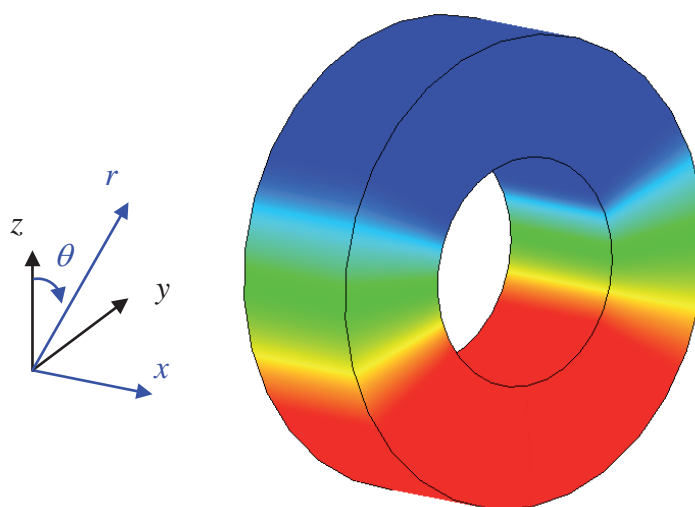


Figure 3: Acoustic Mode Shape Ψ_{010} at $f_{010} = 232\text{Hz}$.

The next step is to use the spectral properties to find the Green’s functions G required in equation (22). The Green’s function is the solution of

$$\nabla^2 G(x, \theta, r | x_o, \theta_o, r_o) + k^2 G(x, \theta, r | x_o, \theta_o, r_o) = -\delta(x - x_o, \theta - \theta_o, r - r_o) \quad (29)$$

with rigid boundary conditions. Note that the dimension of the Dirac delta $\delta(x - x_o, \theta - \theta_o, r - r_o)$ is m^{-3} . The eigenfunctions $\Psi_{qpl}(x, \theta, r)$ satisfy the boundary condition of “rigid wall” given by equation (24). Therefore, these functions are candidates to expand the Green’s function in the domain because the “rigid wall” condition is also required in G .

Then, it is possible to write,

$$G(x, \theta, r | x_o, \theta_o, r_o) = \sum_{q=0}^Q \sum_{p=0}^P \sum_{l=0}^L B_{qpl} \Psi_{qpl}(x, \theta, r) \quad (30)$$

Replacing equation (30) into (29) yields

$$-\sum_{q=0}^Q \sum_{p=0}^P \sum_{l=0}^L B_{qpl} k_{qpl}^2 \Psi_{qpl}(r, \theta, x) + k^2 \sum_{q=0}^Q \sum_{p=0}^P \sum_{l=0}^L B_{qpl} \Psi_{qpl}(x, \theta, r) = -\delta(x - x_o, \theta - \theta_o, r - r_o) \quad (31)$$

The next step is to solve for B_{qpl} by using the orthogonality condition of the acoustic modes shapes Ψ_{qpl} as follow

$$\int_0^{2\pi} \int_0^{L_T} \int_b^a \Psi_{rso}(x, \theta, r) \left[-\sum_{q=0}^Q \sum_{p=0}^P \sum_{l=0}^L B_{qpl} k_{qpl}^2 \Psi_{qpl}(x, \theta, r) + k^2 \sum_{q=0}^Q \sum_{p=0}^P \sum_{l=0}^L B_{qpl} \Psi_{qpl}(x, \theta, r) \right] r dr dx d\theta =$$

$$= -\int_0^{2\pi} \int_0^{L_T} \int_b^a \Psi_{rso}(x, \theta, r) \partial(x - x_o, \theta - \theta_o, r - r_o) r dr dx d\theta$$
(32)

which results in the following expression

$$B_{qpl} \Lambda_{qpl} (k^2 - k_{qpl}^2) = -\Psi_{qpl}(x_o, \theta_o, r_o) \frac{1}{\epsilon_{\mathfrak{S}}}$$
(33)

and

$$B_{qpl} = \frac{\Psi_{qpl}(x_o, \theta_o, r_o) \frac{1}{\epsilon_{\mathfrak{S}}}}{\Lambda_{qpl} (k_{qpl}^2 - k^2)}$$
(34)

Therefore, the Green's function given by equation (30) becomes

$$G(x, \theta, r | x_o, \theta_o, r_o) = \sum_{q=0}^Q \sum_{p=0}^P \sum_{l=0}^L \frac{\Psi_{qpl}(x_o, \theta_o, r_o) \Psi_{qpl}(x, \theta, r) \frac{1}{\epsilon_{\mathfrak{S}}}}{\Lambda_{qpl} (k_{qpl}^2 - k^2)}$$
(35)

This Green's function is symmetric or reciprocal, i.e. $G(x, \theta, r | x_o, \theta_o, r_o) = G(x_o, \theta_o, r_o | x, \theta, r)$ due to the self-adjoint character of the Helmholtz operator and the "rigid wall" boundary condition. Equation (35) is used into (22) to obtain the acoustic pressure due to the boundary motion, $w(r)$ with $r \in \partial\mathfrak{S}$.

2 COUPLED STRUCTURAL-ACOUSTIC PROBLEM

The cavity-structure interaction problem is now solved for this particular problem. Figure 4 illustrates the problem of a structure and the interior acoustic pressure. It is important to remark that the description of the cavity-structural problem is quite complex due to the six indices required to describe the structural and acoustic modes. Here a brief description of the coupled problem will be presented for a general understanding of the solution approach.

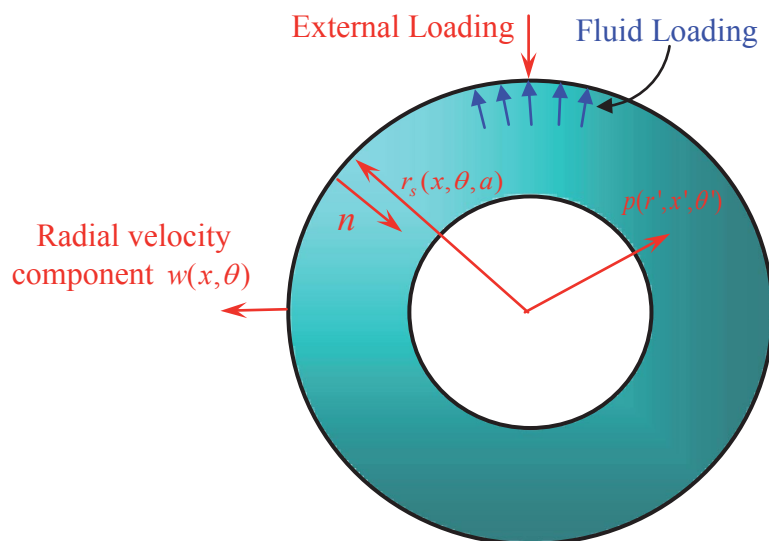


Figure 4: Structure radiating into an enclosed volume.

The approach to solve the coupled problem is to include in the equation of motion of the structure in the force due to the interior pressure i.e. fluid loading. However, the fluid forces depend on the velocity response of the structure which leads to the fluid feedback problem depicted in Figure 5.

The equation of motion of the system including the fluid loading is written as

$$([L_c] - \Omega^2 [I]) \begin{Bmatrix} u \\ v \\ w \end{Bmatrix} = \begin{Bmatrix} f_u \\ f_v \\ f_w \end{Bmatrix} - \begin{Bmatrix} 0 \\ 0 \\ p(x, \theta, a) \end{Bmatrix} \quad (36)$$

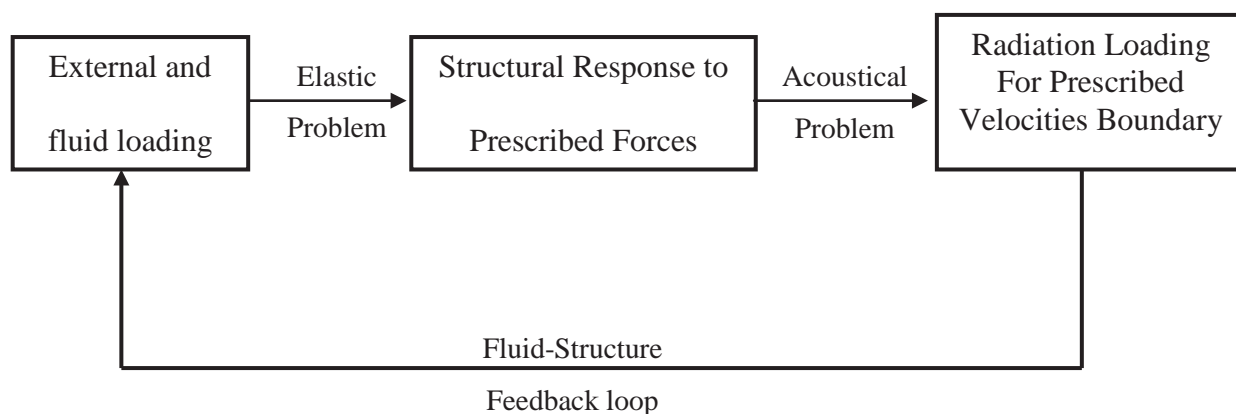


Figure 5: Dynamic interaction between the structure and the fluid.

The forcing function $\{f_u, f_v, f_w\}^T$ in equation (36) is the external force for the harmonic point force assumed for the example. The last vector in (36) represents the acoustic pressure acting on the shell structure. The acoustic pressure, $p(x, \theta, a)$, on the structure is given by equation (22) with G defined in (35)

$$p(x, \theta, a) = \varepsilon_{\bar{\gamma}} \int_0^{L_r} \int_0^{2\pi} i\omega\rho w(x_o, \theta_o) G(x, \theta, a | x_o, \theta_o, a) a \, d\theta_o \, dx_o \quad (37)$$

Where $w(x_o, \theta_o)$ is the radial component of the shell velocity response and $G(x, \theta, r | x_o, \theta_o, a)$ is the Green's function obtained in (35). The solution of the coupled problem is again obtained by expanding the structural response in term of the modes as:

$$\begin{Bmatrix} u \\ v \\ w \end{Bmatrix} = \sum_{m=1}^M \sum_{n=0}^N [\Phi_{mn}] \cdot \begin{Bmatrix} A_{mn}^{(1)} \\ A_{mn}^{(2)} \\ A_{mn}^{(3)} \end{Bmatrix} \quad (38)$$

Where $A_{mn}^{(j)}$ are the structural modal amplitudes including the fluid loading. Then, replacing (38) into (36), it gives

$$\{[L_c] - \Omega^2 [I]\} \sum_{m=1}^M \sum_{n=0}^N [\Phi_{mn}] \begin{Bmatrix} A_{mn}^{(1)} \\ A_{mn}^{(2)} \\ A_{mn}^{(3)} \end{Bmatrix} = \begin{Bmatrix} f_u \\ f_v \\ f_w \end{Bmatrix} - \begin{Bmatrix} 0 \\ 0 \\ p(x, \theta, a) \end{Bmatrix} \quad (39)$$

Once again this equation is pre-multiplied by the transpose of the modal matrix and integrated over the surface of the structure as

$$\int_0^{L_r} \int_0^{2\pi} [\Phi_{rs}]^T \{[L_c] - [\Omega]^2 [I]\} \sum_{m=1}^M \sum_{n=0}^N [\Phi_{mn}] \begin{Bmatrix} A_{mn}^{(1)} \\ A_{mn}^{(2)} \\ A_{mn}^{(3)} \end{Bmatrix} ad\theta dx = \int_0^{L_r} \int_0^{2\pi} [\Phi_{rs}]^T \begin{Bmatrix} f_u \\ f_v \\ f_w \end{Bmatrix} - \begin{Bmatrix} 0 \\ 0 \\ p(x, \theta, a) \end{Bmatrix} ad\theta dx \quad (40)$$

The acoustic pressure acting on the surface of the structure $p(x, \theta, a)$ is obtained from (37) where the radial velocity component is replaced in terms of the structural modes and the modal amplitudes as follow

$$w(x_o, \theta_o) = i\omega \sum_{m=1}^M \sum_{n=0}^N \{W_{mn}^{(1)}, W_{mn}^{(2)}, W_{mn}^{(3)}\} \begin{Bmatrix} A_{mn}^{(1)} \\ A_{mn}^{(2)} \\ A_{mn}^{(3)} \end{Bmatrix} \sin\left(\frac{m\pi}{L_T} x_o\right) \cos(n\theta_o) \quad (41)$$

Then,

$$p(x, \theta, a) = \varepsilon_3 \int_0^{L_r} \int_0^{2\pi} i\omega \rho_A i\omega \sum_{m=1}^M \sum_{n=0}^N \{W_{mn}^{(1)}, W_{mn}^{(2)}, W_{mn}^{(3)}\} \begin{Bmatrix} A_{mn}^{(1)} \\ A_{mn}^{(2)} \\ A_{mn}^{(3)} \end{Bmatrix} \sin\left(\frac{m\pi}{L_T} x_o\right) \cos(n\theta_o) \cdot \sum_q^Q \sum_p^P \sum_l^L \frac{\Psi_{qpl}(x, \theta, a) \Psi_{qpl}(x_o, \theta_o, a)}{\Lambda_{qpl}(k_{qpl}^2 - k^2)} \frac{1}{\varepsilon_3} ad\theta_o dx_o \quad (42)$$

Since only the radial velocity component of the structural response couples with the cavity, the cavity pressure will affect in turn mainly the radial structural modes. Replacing (42) into (40) and solving the integrals explicitly in terms of the unknown modal amplitudes of the radial modes, the following coupled system of equations results

$$[[K_{sr}] - \Omega^2 [M_{sr}]] \cdot \{A_{sr}\} = \{f_{sr}\} - \Omega^2 \sum_{q=0}^Q \sum_{p=0}^P \sum_{l=0}^L [\alpha_{msrqpl}] \cdot \{A_{sr}\} \quad (43)$$

where $[K_{sr}]$ and $[M_{sr}]$ are diagonal matrices and their elements represents the modal stiffness and mass of the radial modes; $\{A_{sr}\}$ is the vector of modal amplitudes; $\{f_{sr}\}$ is the vector of modal forces; and $\sum_{q=0}^Q \sum_{p=0}^P \sum_{l=0}^L [\alpha_{srmnqpl}]$ is the fluid coupling matrix, which requires the manipulation of six indexes. The second term in the right hand side of equation (43) is moved to the other side and the coupled system of equation is solved for the unknown modal amplitudes $\{A_{sr}\}$.

The coefficients α_{srmn} corresponding to the radial component of the matrix $\sum_{q=0}^Q \sum_{p=0}^P \sum_{l=0}^L [\alpha_{srmnqpl}]$ are given by the product of the surface integrals as

$$\alpha_{srmn} = \frac{\int_0^{L_T} \int_0^{2\pi} \Phi_{sr}(x, \theta) \Psi_{qpl}(a, x, \theta) ad\theta dx \int_0^{L_T} \int_0^{2\pi} \Phi_{mn}(x_o, \theta_o) \Psi_{qpl}(a, x_o, \theta_o) ad\theta_o dx_o}{\Lambda_{qpl}(k_{qpl}^2 - k^2)} \quad (44)$$

The coefficient in (44) represents the effect of the (q,p,l) acoustic mode on the (m,n) structural radial mode and reciprocally. One of the advantage of the process developed here is that the interaction of the acoustic and structural modes can be easily determine by inspection of the coefficients in (44). For example, if the coefficient α_{srmn} vanishes implies that the (q,p,l) acoustic does not affect the (m,n) structural mode. It can be observed that the coupling coefficient in (44) is the results of two independent integrations, i.e. in the axial and azimuth directions. Thus, inspection of these integrations can be performed independently. Tables 1 and 2 shows the results of the coupling analysis for the $(0,1,0)$ acoustic mode with several structural modes in the radial and azimuth directions, respectively. In Table 1, the axial pressure variation of the $(0,1,0)$ mode on the shell ($r=a$) and the axial variation of the structural modes are illustrated. From inspection, it is trivial to find that the inner product of these axial variations show that the $(0,1,0)$ acoustic mode will couple with only the $(1,1)$ and $(1,3)$ structural modes.

Table1: Effect in the axial variation on the coupling between structural and acoustic modes of same azimuth variation.


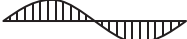






	Structural (m(x), n(θ))		
Acoustic (q(x), p(θ), l(r))			
	(1,1)	(2,1)	(3,1)
(0,1,0)	Coupling $\alpha_{1111010} \neq 0$	No coupling $\alpha_{1212010} = 0$	Coupling $\alpha_{1313010} \neq 0$

Table 2 shows the coupling results on the azimuth direction for the $(0,1,0)$ acoustic mode and the $(1,1)$, $(1,2)$, and $(1,3)$ structural modes. Simple inspection of this table shows that the $(0,1,0)$ mode couples with only the $(1,1)$ structural mode in the azimuth direction. It is easy to find that acoustic and structural modes that have the same azimuth variation will be coupled. Thus, the acoustic mode $(0,1,0)$ can couple with the $(1,1)$, $(3,1)$, $(5,1)$ and so forth.

Table 2: Effect in the circumferential direction on the coupling between structural and acoustic modes.

	Structural (m(x), n(θ))		
Acoustic (q(x),p(θ),l(r))			
	(1,1)	(1,2)	(1,3)
(0,1,0)	Coupling $\alpha_{1111010} \neq 0$	No Coupling $\alpha_{1212010} = 0$	No Coupling $\alpha_{1313010} = 0$

The modal amplitudes for the radial modes are obtained from equation (43), and the structural response is then obtained from (38) and then the acoustic response is computed using (37).

Equation (43) represents the following coupled matrix equation

$$\begin{bmatrix}
 [H_{10}] & [0] & [0] \\
 [0] & [H_{11}] & [0] \\
 \\
 [0] & [0] & [H_{1N}] \\
 \\
 \\
 [H_{20}] & [0] & [0] \\
 [0] & [H_{21}] & [0] \\
 \\
 [0] & [0] & [H_{2N}] \\
 \\
 \\
 \\
 \\
 [H_{M0}] & [0] & [0] \\
 [0] & [H_{M1}] & [0] \\
 \\
 [0] & [0] & [H_{MN}]
 \end{bmatrix}
 \begin{Bmatrix}
 \{A_{10}\} \\
 \{A_{11}\} \\
 \\
 \{A_{1N}\} \\
 \{A_{20}\} \\
 \{A_{21}\} \\
 \\
 \{A_{2N}\} \\
 \\
 \\
 \\
 \{A_{M0}\} \\
 \{A_{M1}\} \\
 \\
 \{A_{MN}\}
 \end{Bmatrix}
 =
 \begin{Bmatrix}
 \{f_{10}\} \\
 \{f_{11}\} \\
 \\
 \{f_{1N}\} \\
 \{f_{20}\} \\
 \{f_{21}\} \\
 \\
 \{f_{2N}\} \\
 \\
 \\
 \\
 \{f_{M0}\} \\
 \{f_{M1}\} \\
 \\
 \{f_{MN}\}
 \end{Bmatrix}
 +
 \Omega^2 \sum_{q=0}^Q \sum_{p=0}^P \sum_{l=0}^L
 \begin{bmatrix}
 [\alpha_{1010qpl}] & [\alpha_{1011qpl}] & [\alpha_{101Nqpl}] & [\alpha_{1020qpl}] & [\alpha_{1021qpl}] & [\alpha_{102Nqpl}] & [\alpha_{10M0qpl}] & [\alpha_{10M1qpl}] & [\alpha_{10MNqpl}] \\
 [\alpha_{1110qpl}] & [\alpha_{1111qpl}] & [\alpha_{111Nqpl}] & [\alpha_{1120qpl}] & [\alpha_{1121qpl}] & [\alpha_{112Nqpl}] & [\alpha_{11M0qpl}] & [\alpha_{11M1qpl}] & [\alpha_{11MNqpl}] \\
 \\
 [\alpha_{1N10qpl}] & [\alpha_{1N11qpl}] & [\alpha_{1N1Nqpl}] & [\alpha_{1N20qpl}] & [\alpha_{1N21qpl}] & [\alpha_{1N2Nqpl}] & [\alpha_{1NM0qpl}] & [\alpha_{1NM1qpl}] & [\alpha_{1NMNqpl}] \\
 [\alpha_{2010qpl}] & [\alpha_{2011qpl}] & [\alpha_{201Nqpl}] & [\alpha_{2020qpl}] & [\alpha_{2021qpl}] & [\alpha_{202Nqpl}] & [\alpha_{20M0qpl}] & [\alpha_{20M1qpl}] & [\alpha_{20MNqpl}] \\
 [\alpha_{2110qpl}] & [\alpha_{2111qpl}] & [\alpha_{211Nqpl}] & [\alpha_{2120qpl}] & [\alpha_{2121qpl}] & [\alpha_{212Nqpl}] & [\alpha_{21M0qpl}] & [\alpha_{21M1qpl}] & [\alpha_{21MNqpl}] \\
 \\
 [\alpha_{2N10qpl}] & [\alpha_{2N11qpl}] & [\alpha_{2N1Nqpl}] & [\alpha_{2N20qpl}] & [\alpha_{2N21qpl}] & [\alpha_{2N2Nqpl}] & [\alpha_{2NM0qpl}] & [\alpha_{2NM1qpl}] & [\alpha_{2NMNqpl}] \\
 \\
 \\
 \\
 [\alpha_{M110qpl}] & [\alpha_{M111qpl}] & [\alpha_{M11Nqpl}] & [\alpha_{M120qpl}] & [\alpha_{M121qpl}] & [\alpha_{M12Nqpl}] & [\alpha_{M0M0qpl}] & [\alpha_{M0M1qpl}] & [\alpha_{M0MNqpl}] \\
 [\alpha_{M210qpl}] & [\alpha_{M211qpl}] & [\alpha_{M21Nqpl}] & [\alpha_{M220qpl}] & [\alpha_{M221qpl}] & [\alpha_{M22Nqpl}] & [\alpha_{M1M0qpl}] & [\alpha_{M1M1qpl}] & [\alpha_{M1MNqpl}] \\
 \\
 [\alpha_{MN10qpl}] & [\alpha_{MN11qpl}] & [\alpha_{MN1Nqpl}] & [\alpha_{MN20qpl}] & [\alpha_{MN21qpl}] & [\alpha_{MN2Nqpl}] & [\alpha_{MNM0qpl}] & [\alpha_{MNM1qpl}] & [\alpha_{MNMNqpl}]
 \end{bmatrix}
 \begin{Bmatrix}
 \{A_{10}\} \\
 \{A_{11}\} \\
 \\
 \{A_{1N}\} \\
 \{A_{20}\} \\
 \{A_{21}\} \\
 \\
 \{A_{2N}\} \\
 \\
 \\
 \\
 \{A_{M0}\} \\
 \{A_{M1}\} \\
 \\
 \{A_{MN}\}
 \end{Bmatrix}
 \quad (45)$$

Where in the last equation

$$[H_{sr}] = [[K_{sr}] - \Omega^2 [M_{sr}]] \quad (46)$$

3 NUMERICAL EXAMPLE

A numerical simulation for the coupled acoustic cavity-shell structural model will be presented. The in vacuo and coupled responses were computed and compared over the frequency range of 0-400 Hz. The analysis included 25 structural modes and 5 acoustic modes. Figure 6 and 7 show the modal amplitudes for the $\Phi_{11}^{(1)}$ and $\Phi_{31}^{(1)}$ radial structural modes with and without acoustic coupling, respectively. The structural radial mode $\Phi_{11}^{(1)}$, and the acoustic mode Ψ_{010} are coupled as shown in these figures. Table 3 shows the acoustic cavity resonance frequencies for a range between 0 to 1000 Hz. The acoustic natural

frequency for the mode Ψ_{010} is highlighted in the table because is the only acoustic mode in the frequency range of interest for the example that couples with the structure dynamics.

The in vacuo and coupled responses were computed and compared over the frequency range of 0-400 Hz. The analysis included 25 structural modes and 5 acoustic modes. Figure 6 and 7 show the modal amplitudes for the $\Phi_{11}^{(1)}$ and $\Phi_{31}^{(1)}$ radial structural modes with and without acoustic coupling, respectively. The structural radial mode $\Phi_{11}^{(1)}$, and the acoustic mode Ψ_{010} are coupled as shown in these figures.

Table 3: Acoustic cavity natural frequencies between [0-1000] Hz

q	p	l	frequency [Hz]
0	0	0	0.0
0	1	0	232.6
0	2	0	465.1
0	3	0	697.6
1	0	0	879.5
1	1	0	909.7
0	4	0	930.2
1	2	0	994.9

It is clear that the effect of the acoustic cavity mode in the structural response is significant even though the acoustic resonance is not very close to the structural resonance, i.e. not tuned. Since the acoustic system is modeled without acoustic damping, the “slight” damping in the acoustic resonance is coming from the shell structure due to the coupling process. It can be observed that this small amount of damping do not help enough to control the effect of the acoustic cavity in the modal amplitude response, i.e., Figure 6 and 7.

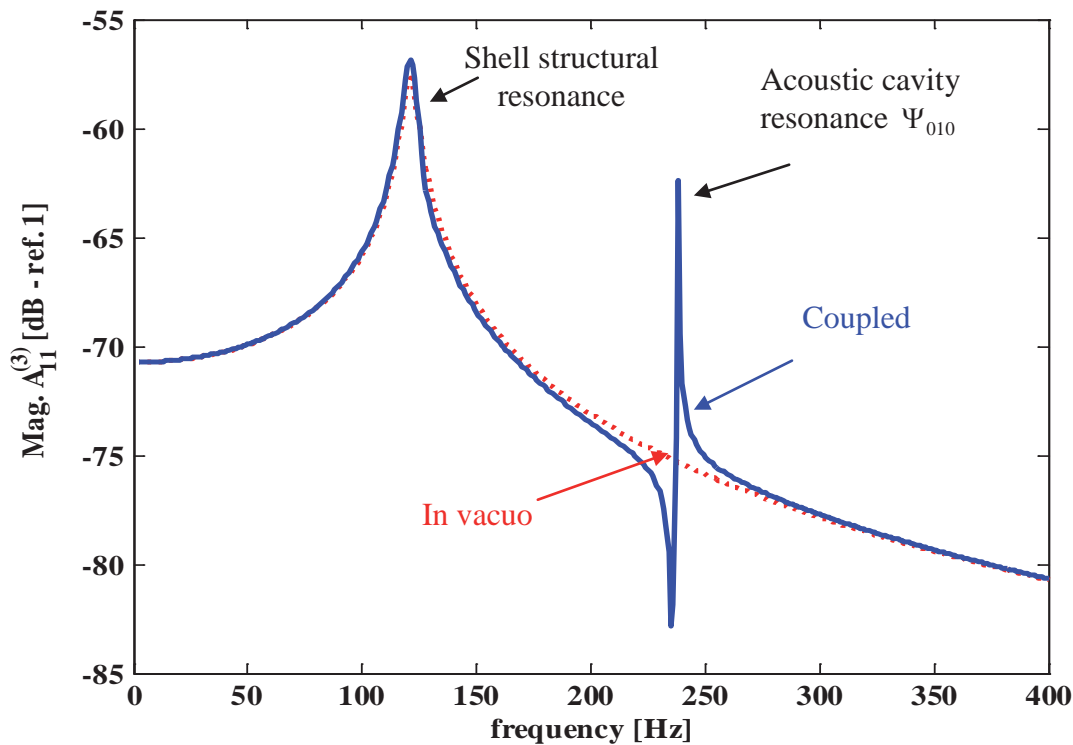


Figure 6: Radial Modal Amplitude for mode $\Phi_{11}^{(1)}$.

It is interesting to note that the relatively high damping of the shell structure does not damp out the energy in the acoustic resonance. Figure 7 also reveals the coupling of the structural modes $\Phi_{11}^{(1)}$ and $\Phi_{31}^{(1)}$ by the acoustic mode.

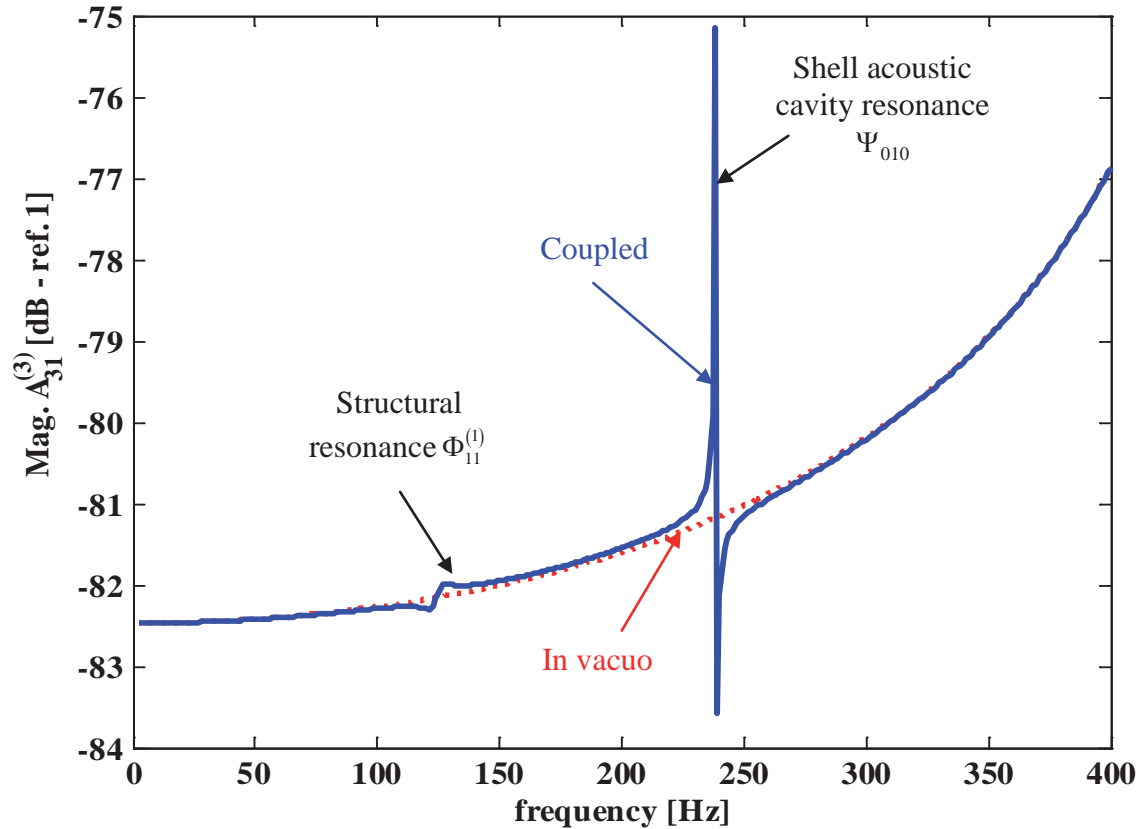


Figure 7: Radial Modal Amplitude for mode $\Phi_{31}^{(1)}$.

Figure 8 includes three curves corresponding to the in vacuum model in red dotted line, the coupled model in blue solid line, and results from a test measurement performed by Yamauchi and Akiyoshi (2002) in a green dash-dotted line.

The gain factor to match the acoustic cavity resonances is 0.1775 . The results from this simple analytical model show qualitatively similar trends as the experimental observation, i.e. blue line for coupled and green line for experimental results. The green line corresponding to the experimental data shows also the presence of the rigid body motion, which is not accounted for the model.

The dynamic of the shell structure is clearly represented and the effect of the acoustic cavity is very well predicted. These results provide a validation of the close model approach undertaken here as a valid tool to capture the behavior of the shell dynamics including the acoustic cavity.

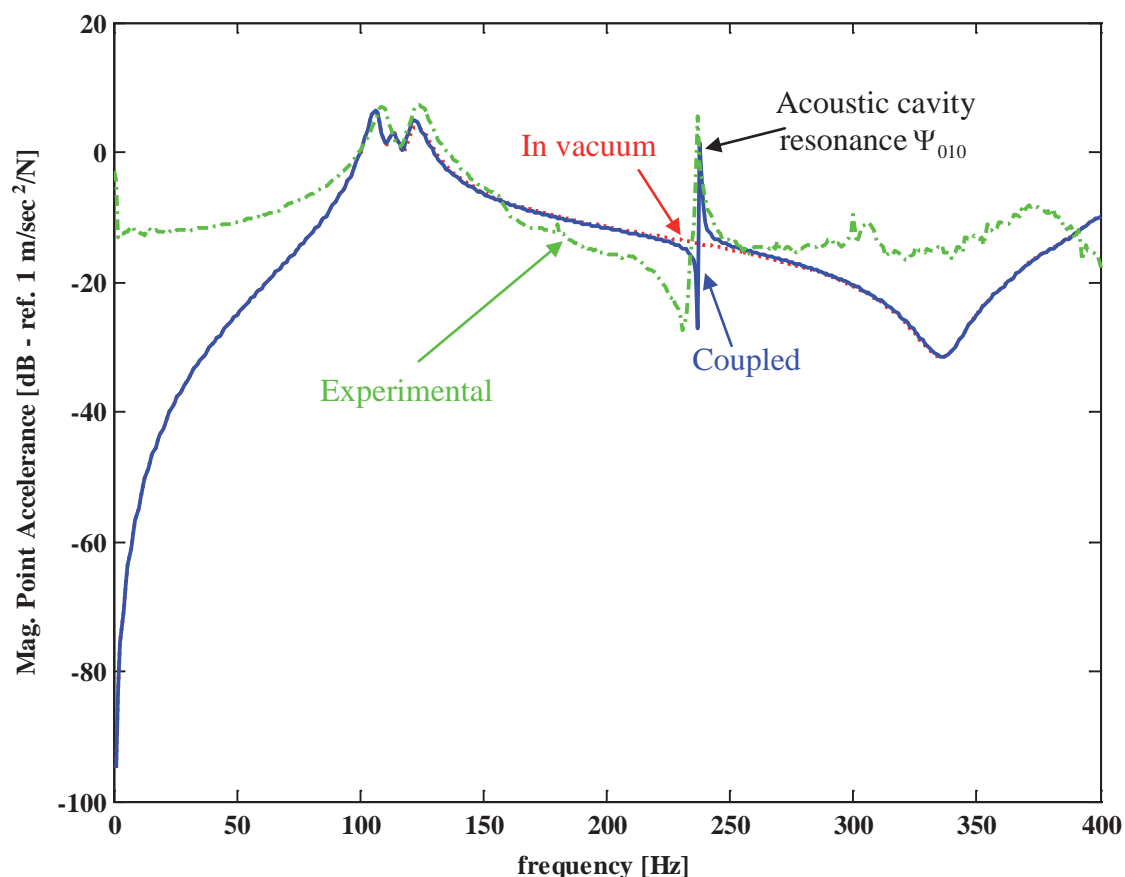


Figure 8: Point acceleration at the external force location at the shell middle point.

SYNOPSIS AND CONCLUSIONS

The study presented here shows analytical closed form solutions to help gaining insight into the coupling phenomenon between the acoustic cavity and a structural enclosure. Subsequently the analysis permits the investigation and development of practical techniques to control the cavity resonance. In the example developed in this work, the external excitation is a harmonic point force acting normal to the external surface of the structural enclosure. Therefore, numerical results for the cavity-structural model are shown. Lastly, validation of the structural shell model is also included by comparison with experimental results obtained from the experimental work done by Yamauchi and Akiyoshi (2002).

REFERENCES

- Akerberg, P. M., Jansen, B. H., & Finch, R. D. (1995). Neural net-base monitoring of steel beam. *Journal of the Acoustical Society of America*, 98 (3), 1505–1509.
- Bishop, C. M. (1995). *Neural Networks for Pattern Recognition*. Oxford University Press.
- Chang, C., Chang, T., & Wang, M. (2000). Structural damage detection using an iterative neural network. *Journal of Intelligent Material Systems and Structures*, 11, 32–42.

- Chen, D., & Wang, W. (2002). Classification of wavelet map patterns using multi-layer neural networks for gear fault detection. *Mechanical systems and signal processing*, 16 (4), 695–704.
- Ewins, D. J. (1986). *Modal Testing: Theory and Practice*. Research Studies Press Ltd.
- Fang, X. L., & Tang, J. (2005). Structural damage detection using neural network with learning rate improvement. *Computers and Structures* (83), 2150–2161.
- Fukunaga, K. (1990.). *Introduction to Statistical Pattern Recognition*. Academic Press,.
- Haykin, S. (1999). *Neural networks a comprehensive foundation*. Prentice Hall.
- Haykin, S. (2009). *Neural networks and learning machines* (3rd. edition, ed.). Prentice Hall.
- Man, X. C., McClure, L. M., Wang, Z., Finch, R. D., Robin, P. Y., & Jansen, B. H. (1994). Slot depth resolution in vibration signature monitoring of beams using frequency shift. *Journal of the Acoustical Society of America*, 95 (4), 2029–2037.
- Ripley, B. D. (1995). *Pattern Recognition and Neural Networks*. Cambridge University Press.
- Rojas, R. (1996). *Neural Networks - A Systematic Introduction*. Springer-Verlag.
- Sun, Z., & Chang, C. (2002). Structural damage assessment based on wavelet packet transform. *Journal of Structural Engineering*, 128 (10), 1354–1361.
- Zang, C., & Imregun, M. (2001). Structural damage detection using artificial neural networks and measured frf data reduced by principal component projection. *Journal of Sound and Vibration*, 24 (5), 813–827.